Synthesis of brightly luminescent colloidal formamidinium lead bromide perovskite $FAPbBr_3$ nanoplatelets with tunable emission

Nabila Jarmouni[1, 2*], *Marco* Tomaiuolo[2], *Alessio* Gabbani[3,4], *Francesco* Pineider[2], *Rajaa* Bassam[1], *Said* Belaaouad[1], *Said* Benmokhtar[1]

[1]University Hassan II of Casablanca, Faculty of sciences Ben M'sik, Department of Chemistry, Laboratory of Physical Chemistry of Materials, Casablanca, Morocco
[2]Universityof Pisa, Department of Chemistry and Industrial Chemistry, Pisa, Italy
[3]Italian National Council for Research - Institute for the Chemistry of OrganoMetallic Compounds, Florence, Italy
[4]University of Florence, Department of Chemistry"U. Schiff", Florence, Italy
* Corresponding author*:* nabilajarmouni@gmail.com

Abstract Hybrid halide perovskites are semicondoctor materials with desirable characteristics of color-tunable and narrow-band emissions for lighting and display technology. They have size-tunable emissions due to quantum size effects. In this work, the Formamidinium Lead Bromide perovskite $CH(NH_2)_2PbBr_3$ nanoplatelets (NPLs) were successfully synthesized by ligand-assisted reprecipitation method under room condition, in which the emission color-tunability was realized via quantum size effect without anion–halide mixing, by varying the oleylamine to oleic acid volume ratio as surfactants, while the total amount of oleic acid remained unchanged. We are able to adjust the optical proprieties of $FAPbBr_3$ NPLs and, consequently, their structural properties. The obtained colloidal solutions of $FAPbBr_3$ nanoplatelets with uniform size exhibited different photoluminescence wavelengths covering the spectral region from 440 to 525 nm. The maximum absolute PL quantum yield (PLQY) of the green emission was measured to be as high as 80% at room temperature. The size of FAPbBr3 NPLs could be effectively tuned from 15.5 to 38.1 nm with an increase in the oleylamine and oleic acid ligands ratio.

1. Introduction

Recently, lighting and display technologies are seeking emitter materials with the ability to precisely fine-tune the emission wavelength with narrow FWHM, to improve the color performance of lighting and display systems [1]. Among various emitter materials, lead halide perovskites NCs have attracted great attention due to their excellent performance, including precisely tunable narrow emission spectrum across the visible region, high photoluminescence quantum yields (PLQYs), as well as high stability [2–4]. On the other hand, this class of materials has already shown great potential in many areas, such as solar cells [5], lasers [6], and advanced photonics [6], owing to not only their exceptional optoelectronic properties but also their lower cost and more simple synthesis compared to the state of the art semiconductor materials. Lead halide perovskite nanocrystals (NCs) are receiving a lot of attention in the early, due to their exceptionally high photoluminescence quantum yields reaching almost 100% and tunability of their optical band gap over the entire visible spectral range by modifying composition or dimensionality/size.

Hybrid halide perovskites NCs are a new type of perovskite semiconductor material where the structure contains an organic and metal cation, which can have the properties of organic semiconductors as well as those of the inorganic. Their typical crystal structure is illustrated in Figure 1, where A is a monovalent cation such as methylammonium (CH_3NH^+; MA^+) or formamidinium ($CH(NH_2)_2^+$; FA^+) positioned at the center, B is a divalent metal cation (Pb^{2+}) at the center of the octahedra, and X is a halide anion (Cl^-, Br^-, or I^-) that occupies the corner-sharing BX_6 octahedra (Figure 1). These components not only dictate the crystal structure but also control their optical and electronic properties. Their optical properties can be significantly tuned by varying the composition. While the bivalent cation (Pb) and halide (X) strongly affect the optical properties, which can be tuned throughout the visible range by controlling the halide content. the variation of the monovalent cation (A+) only leads to minimal changes [7]. However, the type of monovalent cation can greatly influence the stability and PLQY of hybrid perovskite nanocrystals [3]. Among these perovskites, formamidinium lead halide perovskite nanocrystals ($FAPbX_3$ NCs) exhibit a variety of attractive properties comparable to other Lead halide perovskites NCs, making it one of the most attractive perovskite

NCs materials for lighting and display sources [8–13]. Their PL emission can be easily adjusted not only through size control, and subsequently through quantum confinement, as in the case of standard quantum dots, but also through compositional mixing, for example via simple anion exchange reactions [14], obtaining broadly tunable photoluminescence (PL) from the ultraviolet (UV) to the near-infrared region of the electromagnetic spectrum. The manipulation of the morphology and optical and electronic properties of perovskite NCs can be easily customized by precisely controlling the experimental conditions like varying the temperature of the nonpolar solvent or the reaction [15], the precursor and ligand concentrations [7,16–18], or the ratio of the perovskite precursor[19].

In this contribution, the emission tuning of Formamidinium Lead Bromide perovskite $FAPbBr_3$ nanoplatelets (NPLs) was achieved by varying the starting ligand volume ratio (oleylamine, OAm, and oleic acid, OA). The NPLs were synthesized via the ligand-assisted reprecipitation method at room temperature (Figure 2)[1].

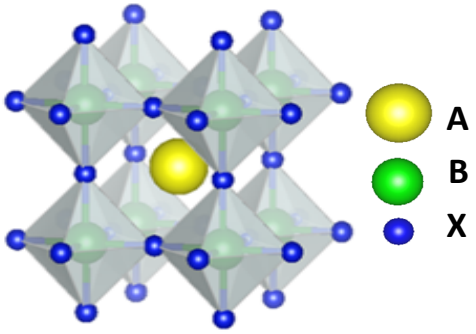

Figure 1: Illustration of the perovskite crystal structure

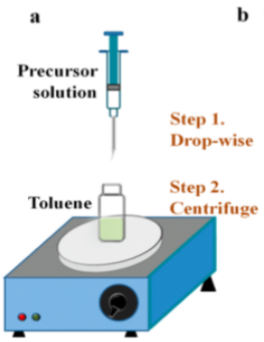

Figure 2: Schematics of ligand-assisted re-precipitation (LARP) method used to produce $FAPbBr_3$ NCs[1]

2. Experimental section

2.1. Materials.

Formamidine acetate salt ($HN{=}CHNH_2{\times}CH_3COOH$, 99%), lead (II) bromide ($PbBr_2$, 99.999% trace metals basis), N, N-dimethylformamide (DMF, 99.8%), hydrobromic acid (HBr, 48% in water, 99.99%), Oleylamine **OAm** (primary amine 98%) oleic acid **OA** (90%), acetonitrile (CH_3CN, 99.8%), chloroform (>99%), toluene (>99%), hexane (95%), diethyl ether (99.9%) were purchased from Sigma-Aldrich.

2.2. Synthesis of Formamidinium bromide (FABr)

Formamidinium bromide (FABr) was synthesized by neutralizing 2 molar excesses (1:2 ratio) of a 48% aqueous hydrobromic acid with formamidinium acetate salt to obtain the full protonation of the amine precursor. 0.1 mol of formamidinium acetate powder was slowly dissolved in 0.2 mol of 48% hydrobromic acid. The mixture was stirred for 1 hour in a round-bottom flask, which was kept in an ice bath. The FABr solid was formed by removing the solvent in a rotary evaporator at 70°C. This was then washed several times with diethyl ether and recrystallized twice with ethanol, to form white crystals. The white crystalline material was then dried at 80°C overnight in a vacuum oven before further use.

2.3. Synthesis of Formamidinium lead bromide perovskite nanoplates ($FAPbBr_3$)

The synthesis of colloidal $CH(NH_2)_2PbBr_3$ NCs was performed via the ligand-assisted reprecipitation method at room temperature in the open air. Typically, 0.1 mmol of FABr and 0.1 mmol of lead bromide $PbBr_2$ were dissolved in 1 ml DMF forming 0.1 mM of the solution. The mixture was stirred until completely dissolved. Then, different OA to OLM volume ratios 10:5; 10:4; 10:3; 10:2 were added to achieve different emission wavelengths. The mixture was stirred until a clear solution was obtained. Next, 100 µL of this mixture was rapidly injected into 3 ml of chloroform under vigorous stirring. A bright yellow color colloidal solution appeared within seconds, indicating the formation of the perovskite NCs, due to their extremely fast ionic nature of the metathesis, nucleation, and growth kinetics. Noted that the concentration of yellow color decrease when the OAm volume increase in solution.

The resulting NCs were precipitated with a mixture of acetonitrile/toluene (1:1), followed by centrifugation at 900 rpm for 5 min. The precipitate was then redispersed in hexane using mild sonication to form a stable colloidal dispersion under ambient conditions. In this crystallization method of perovskite nanocrystals (illustrated in Figure 2), the injection of perovskite precursors with organic ligands (OA,OAm) in a polar solvent such as DMF into a non-polar solvent such as chloroform changed the solubility of the precursors in solution. The interplay between good solvent and poor solvent mixing produces a highly supersaturated state immediately and then induces fast nucleation and growth of perovskite nanocrystals [1].

2.4. Characterization methods

UV-VIS absorption and Photoluminescence (PL) measurements

The UV-Vis absorption spectroscopy was recorded at room temperature using Cary 5000 spectrophotometer (Agilent, Santa Clara, CA, USA). The PL spectra were measured at room temperature using an excitation wavelength (λex) of 350 nm on a Fluorolog-3 spectrofluorometer (Horiba Jobin–Yvon, Horiba Italy, Rome, Italy) equipped with a 450 W xenon arc lamp and double-grating excitation and single-grating emission monochromators. The photoluminescence quantum yield was determined according to the method described by de Mello et al[20]. by using a 152 mm diameter "Quanta-ϕ" integrating sphere [21], fitted to the spectro-fluorimeter. The sample was prepared by diluting the dispersion solution of NPLs in hexane, in quartz cuvettes with a path length of 1 cm.

Transmission Electron Microscopy (TEM) characterization

TEM measurement was performed on a JEOL-100 SX transmission electron microscope operating at an acceleration voltage of 100 kV. The Sample for TEM was prepared by drop-casting a dilute solution of NPLs in hexane onto a standard copper grid coated with a continuous amorphous carbon film. The size distribution of NPLs was obtained from the TEM images with ImageJ software.

X-ray Powder Diffraction (XRPD)

Powder XRD analysis was carried out using a Bruker D8 Advance diffractometer equipped with CuKα radiation and operating in θ–θ Bragg Brentano geometry at 40 kV and 40 mA. A concentrated solution of the NPLs in hexane was drop casted onto a zero-background silicon wafer and dried at room temperature for measurement.

3. Results and discussion

3.1. Optical characterizations

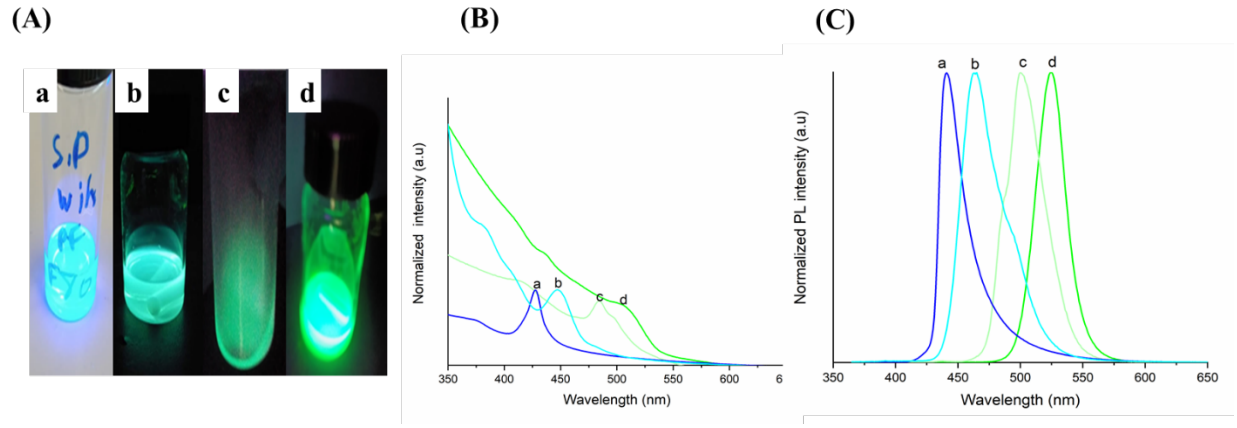

Figure 3: a) Digital photos of the $FAPbBr_3$ NPLs dispersed in Hexane under the illumination of 365 nm, and the corresponding (b) PL and (c) absorption spectra. The $FAPbBr_3$ NPLs were synthesized by using different ratios of Oleic acid (OA)/Oleylamine (OAm) volume :(a) 10:5; (b) 10:4; (c) 10:3; (d)10:2.

As shown in the digital photos (Figure 3A) of the different-emission color of as-prepared $FAPbBr_3$ NPLs dispersed in

hexane under illumination at 365 nm at room temperature, synthesized with different Oleic acid (OA)/Oleyamine (OAm) volume ratio :(a) 10:5; (b) 10:4; (c) 10:3; (d)10:2. This enables precise tuning of the absorption edge and photoluminescence (PL) of the NPLs from blue to green color.
The optical color of the colloidal $FAPbBr_3$ NPLs can be tuned from green to blue by increasing Oleylamine volume. To quantify these observations, absorption and photoluminescence (PL) spectroscopies were performed (Figures 3B and 3C). The ligand ratio control allowed to adapt the emission color of the platelet-like $FAPbBr_3$ NCs, leading to shifting of the band−band absorption edge (Figure 3B) and the PL band (Figure 3C). The measured PL spectra are blue-shifted from 525 to 440 nm (2.36 eV- 2,81 eV) with the increasing OAm content. The sample synthesized with 10:2 volume ratio exhibits a green emission at 525 nm with narrow FHWM about 29nm, and high PL quantum yield (PLQY) approximately 80% at room temperature.
As shown in Figure. 3B, an obvious blue shift of the absorption band is observed. It should be noted that the absorption peak changes gradually from sharp to less distinct with an increase of the mean size, which is similar to that observed in other colloidal QDs systems including CdSe and CdTe QDs [22].
Such a gradual blueshift indicates quantum confinement effect in $FAPbBr_3$ NPLs, which could be further confirmed using TEM image analysis.

3.2. Structural characterizations

TEM micrographs were acquired to study the size and morphology of the resulting perovskite nanocrystals synthesized by using different oleic acid/oleylamine volume ratios, and the corresponding TEM images are depicted in figure 5. The perovskite NCs exhibit a platelet shape with a narrow size distribution.

The mean size in the range of 38 to 15 nm increases with the oleylamine volume. The platelets were not separated but instead stacked on top of each other, which can also be seen by the varying contrast in the image.

As the size of the nanocrystals approaches the exciton Bohr radius of the material, quantum confinement effects start to influence the excitonic wave function and the energetic states of the exciton, leading to blue-shifted photoluminescence (Figure. 3C). As already mentioned above, the optical properties of perovskite NCs strongly depend not only on their constituent metal and halide ions but also on their dimensionality and size. These NPLs perovskites show quantum confinement effects analogous to conventional semiconductors when their dimensions are reduced to sizes comparable to their respective exciton Bohr radii [2,13].

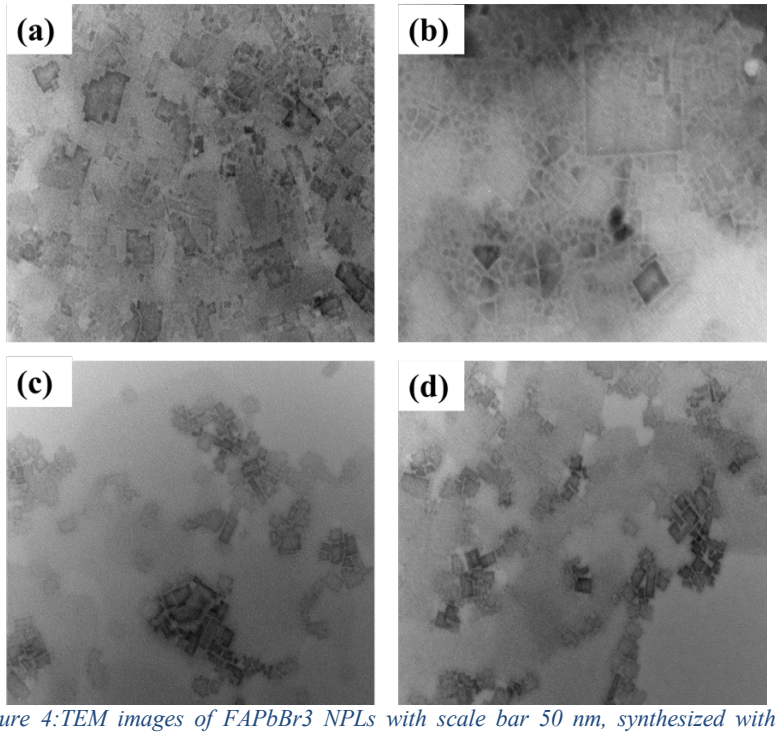

Figure 4:TEM images of FAPbBr3 NPLs with scale bar 50 nm, synthesized with different OAm/OA volume ratio: :(a) 10:5; (b) 10:4; (c) 10:3; (d)10:2.

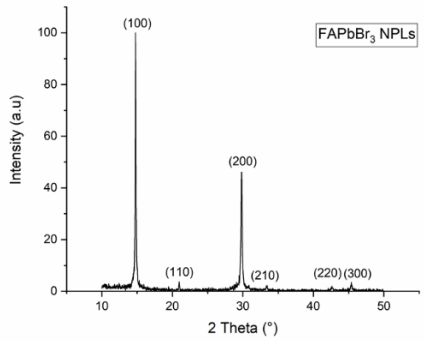

Figure5: XRD pattern of $FAPbBr_3$ NPLs synthesized with OA/OAm 10:2 volume ratio

To further confirm the crystal structure, the XRD pattern was employed to study the crystal structure of the $FAPbBr_3$ perovskite NPLs, Figure 4. presents the XRD patterns of the NPLs with a mean size of 38.1 nm, showed that $FAPbBr_3$ have crystalline structures that can be assigned to the perovskite crystal phase.

The perovskite crystalline structure was confirmed by comparing nanoplates diffractogram with bulk $FAPbBr_3$ diffraction patterns (JCD 87-0158); the $FAPbBr_3$ nanoplates possessed a cubic phase (space group Pm-3m, no. 221) similar to that of the reported bulk crystals with the unit cell parameter of a= 5.9944 A . We found that our results are in excellent agreement with the previous reports by Li, Feiming, et al [10]. $FAPbBr_3$ gave diffraction peaks at 14.6°, 20.7°, 29.5°, 33.3°, 36.5°, 42.4°, and 45.2° 2θ which correspond to the reflections from the lattice planes (100), (110), (200), (210), (211), (220) and (300) respectively, in agreement with the cubic phase $FAPbBr_3$ with Pm-3m space group as reported in previous literature.

Conclusion

In summary, we demonstrate the color emission-tunability of $FAPbBr_3$ perovskite nanoplatelets (NPLs) by varying the ratio of oleic acid and oleylamine volume, while the total amount of oleic acid remained unchanged. By adjustable the optical proprieties of $FAPbBr_3$ NPLs, we achieved changing size and the morphology of the NPLs. We find that as the content of OAm in the precursor suspension is increased, the size of the produced nanoplatelets is reduced. Due to quantum confinement effects, the emission color could be readily tuned from green to blue with the corresponding emission peaks covering the spectral range from 525 to 440 nm. These optical characteristics of the obtained $FAPbBr_3$ perovskite NPLs are comparable with the classical semiconductor QDs such as CdSe and CdTe, thus the perovskite may be a cheaper, high-performance alternative to CdSe or CdTe QDs.

References:

1. F. Zhang, H. Zhong, C. Chen, X. G. Wu, X. Hu, H. Huang, J. Han, B. Zou, and Y. Dong, ACS Nano **9**, 4533 (2015)
2. L. Polavarapu, B. Nickel, J. Feldmann, and A. S. Urban, Advanced Energy Materials **7**, (2017)
3. D. Chen and X. Chen, Journal of Materials Chemistry C **7**, 1413 (2019)

4. T. Chiba and J. Kido, Journal of Materials Chemistry C **6**, 11868 (2018)
5. S. D. Stranks and H. J. Snaith, Nature Nanotechnology **10**, 391 (2015)
6. S. Colella, M. Mazzeo, A. Rizzo, G. Gigli, and A. Listorti, Journal of Physical Chemistry Letters **7**, 4322 (2016)
7. J. A. Sichert, Y. Tong, N. Mutz, M. Vollmer, S. Fischer, K. Z. Milowska, R. García Cortadella, B. Nickel, C. Cardenas-Daw, J. K. Stolarczyk, A. S. Urban, and J. Feldmann, Nano Letters **15**, 6521 (2015)
8. L. Protesescu, S. Yakunin, M. I. Bodnarchuk, F. Bertolotti, N. Masciocchi, A. Guagliardi, and M. v. Kovalenko, Journal of the American Chemical Society **138**, 14202 (2016)
9. D. Yu, F. Cao, Y. Shen, X. Liu, Y. Zhu, and H. Zeng, *Dimensionality and Interface Engineering of 2D Homologous Perovskites for Boosted Charge Carrier Transport and Photodetection Performances* (2017)
10. F. Li, L. Yang, Z. Cai, K. Wei, F. Lin, J. You, T. Jiang, Y. Wang, and X. Chen, Nanoscale **10**, 20611 (2018)
11. T. Zhang, H. Li, P. Yang, J. Wei, F. Wang, H. Shen, D. Li, and F. Li, Organic Electronics **68**, 76 (2019)
12. L. Fan, K. Ding, H. Chen, S. Xiang, R. Zhang, R. Guo, Z. Liu, and L. Wang, Organic Electronics **60**, 64 (2018)
13. H. Ma, M. Imran, Z. Dang, and Z. Hu, Crystals **8**, 182 (2018)
14. M. Imran, V. Caligiuri, M. Wang, L. Goldoni, M. Prato, R. Krahne, L. de Trizio, and L. Manna, Journal of the American Chemical Society **140**, 2656 (2018)
15. H. Huang, A. S. Susha, S. v. Kershaw, T. F. Hung, and A. L. Rogach, Advanced Science **2**, (2015)
16. I. Levchuk, P. Herre, M. Brandl, A. Osvet, R. Hock, W. Peukert, P. Schweizer, E. Spiecker, M. Batentschuk, and C. J. Brabec, Chemical Communications **53**, 244 (2017)
17. I. Levchuk, A. Osvet, X. Tang, M. Brandl, J. D. Perea, F. Hoegl, G. J. Matt, R. Hock, M. Batentschuk, and C. J. Brabec, Nano Letters **17**, 2765 (2017)
18. D. N. Minh, J. Kim, J. Hyon, J. H. Sim, H. H. Sowlih, C. Seo, J. Nam, S. Eom, S. Suk, S. Lee, E. Kim, and Y. Kang, Chemistry of Materials **29**, 5713 (2017)
19. L. Peng, A. Tang, C. Yang, and F. Teng, Journal of Alloys and Compounds **687**, 506 (2016)
20. Dr. H. F. W. R. H. F. Dr. John C. de Mello, Advanced Materials (2004)
21. L. Porrès, A. Holland, L. O. Pålsson, A. P. Monkman, C. Kemp, and A. Beeby, in *Journal of Fluorescence* (Springer Science and Business Media Deutschland GmbH, 2006), pp. 267–273
22. Y. M. Huang, K. J. Singh, A. C. Liu, C. C. Lin, Z. Chen, K. Wang, Y. Lin, Z. Liu, T. Wu, and H. C. Kuo, Nanomaterials **10**, 1 (2020)